ELSEVIER

PII: S0032-3861(97)00124-9

Polymer Vol. 38 No. 23, pp. 5823–5833, 1997

0032-3861/97/$17.00+0.00

On the preparation of acrylic acid/vinyl acetate copolymers with constant composition: 4. Modelling batch and continuous free-radical AA/VA copolymerization

Carmen Zaldívar, Gerardo Iglesias and Octavio del Sol
Laboratorio de Polímeros, Dirección de Química CNIC, Centro Nacional de Investigaciones Científicas, PO Box 6880, Habana, Cuba

and José Carlos Pinto*
Programa de Engenharia Química/COPPE, Universidade Federal do Rio de Janeiro, Cidade Universitária CP: 68502, Rio de Janeiro, 21945-970 RJ, Brazil
(Received 29 January 1997)

A detailed mathematical model is developed to describe the solution copolymerization of acrylic acid (AA) and vinyl acetate (VA) in batch and continuous stirred tank reactors. Lacking kinetic parameters are then estimated, based on batch experimental data. To validate the model, experiments are carried out in continuous reactors, showing that model predictions are good in all conditions analysed. The model is then used to design operation conditions where AA/VA copolymers with uniform composition can be produced with small average AA block sizes. © 1997 Elsevier Science Ltd.

(Keywords: acrylic acid; vinyl acetate; copolymerization)

INTRODUCTION

Copolymers of acrylic acid (AA) and vinyl acetate (VA) find successful applications in the mineral, textile, cosmetics, paper and oil industries and are also used as adhesives and for improving soil and water quality[1,2]. More recently, the use of acrylic acid/vinyl acetate copolymers is also being considered in certain processes which require precise control of copolymer composition, so that developing and implementing kinetic models is of great importance to allow the precise determination of the operation conditions needed to meet certain product specifications.

Although there is a lack of kinetic data regarding the AA/VA copolymerizations, it is well known that these systems are characterized by very different reactivity ratios ($r_1 = 10.0, r_2 = 0.01$)[3], ($r_1 = 2.5, r_2 = 0.04$)[4], which makes it difficult to control the copolymer composition in batch reactions. Heublein and coworkers[5–10] developed a technique for producing homogeneous AA/VA copolymers, with composition ranging from 5% to 90% of AA, which comprises the free-radical polymerization of AA/VA mixtures in buffered methanol/water solutions. According to the results obtained in our laboratories[11], though, copolymer properties were found to be too sensitive to process perturbations, so that alternative reaction schemes are under study[12]. Special attention has been given to semicontinuous and continuous free-radical polymerizations in ethanol/water solutions.

The main objectives of this paper are carrying out AA and VA homopolymerizations and AA/VA copolymerizations in azeotropic solutions of ethanol and water (ETOH) at 75°C, in batch reactors, estimating the kinetic constants based on monomer conversion and polymer composition data, and building a kinetic model to allow the development of suitable operation conditions to meet certain product specifications in continuous reactors. Simulation results are validated by performing independent continuous copolymerization reactions at different residence times and monomer feed concentrations.

EXPERIMENTAL

Acrylic acid was bought from Carlo Erba, vinyl acetate was bought from Hoechst and benzoyl peroxide was bought from Merck. The other chemical species were commercial grades available in Habana. All liquid reagents were purified through distillation. Benzoyl peroxide was purified through recrystallization in methanol. Polymerizations were initiated by benzoyl peroxide and were carried out in 50 ml stirred tank reactors, under nitrogen atmosphere, at 75°C. Monomer conversions were evaluated gravimetrically, by drying the polymer mass in vacuum ovens at ambient temperature. Copolymer compositions were evaluated through potentiometric titration with NaOH in solutions of NaCl 0.05 M. The homogeneity of final polymer product was analysed by preparing an initial polymer solution in methanol and separating polymer fractions which precipitate after the repeated addition of specified amounts of

* To whom correspondence should be addressed

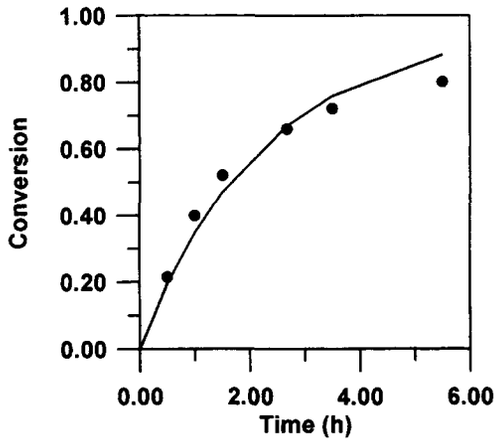

Figure 1 Monomer conversion for VA homopolymerization in ETOH. ($M_{20} = 3.25\,\text{gmol}\,l^{-1}$, $ci_0 = 0.0125\,\text{gmol}\,l^{-1}$)

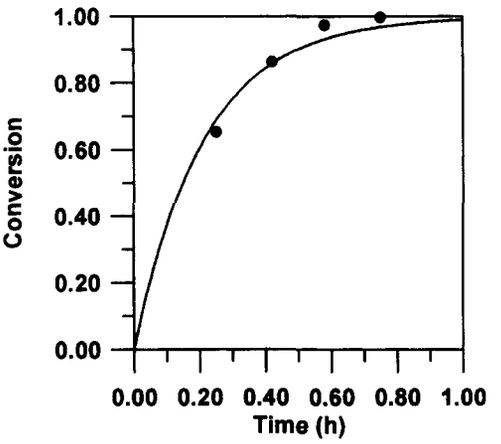

Figure 4 Monomer conversion for AA homopolymerization in ETOH. ($M_{10} = 4.33\,\text{gmol}\,l^{-1}$), $ci_0 = 0.0095\,\text{gmol}\,l^{-1}$)

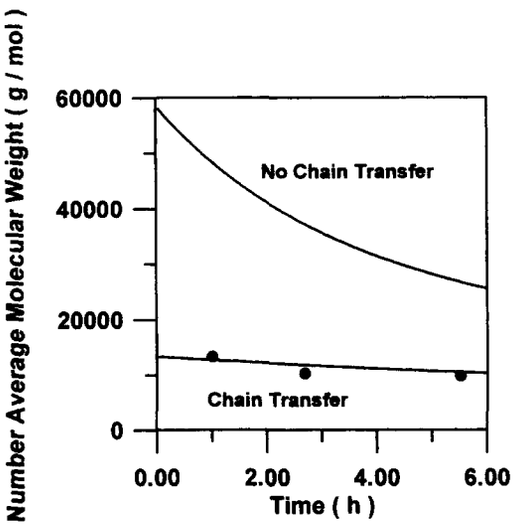

Figure 2 Number average molecular weight for VA homopolymerization in ETOH. ($M_{20} = 3.25\,\text{gmol}\,l^{-1}$, $ci_0 = 0.0125\,\text{gmol}\,l^{-1}$)

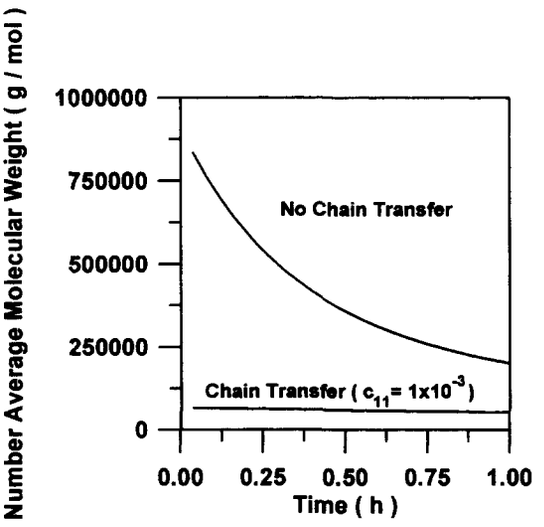

Figure 5 Number average molecular weight for AA homopolymerization in ETOH. ($M_{10} = 4.33\,\text{gmol}\,l^{-1}$, $ci_0 = 0.0095\,\text{gmol}\,l^{-1}$)

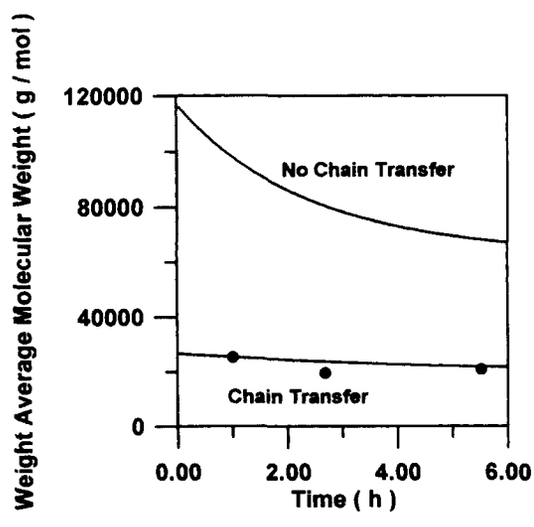

Figure 3 Weight average molecular weight for VA homopolymerization in ETOH. ($M_{20} = 3.25\,\text{gmol}\,l^{-1}$, $ci_0 = 0.0125\,\text{gmol}\,l^{-1}$)

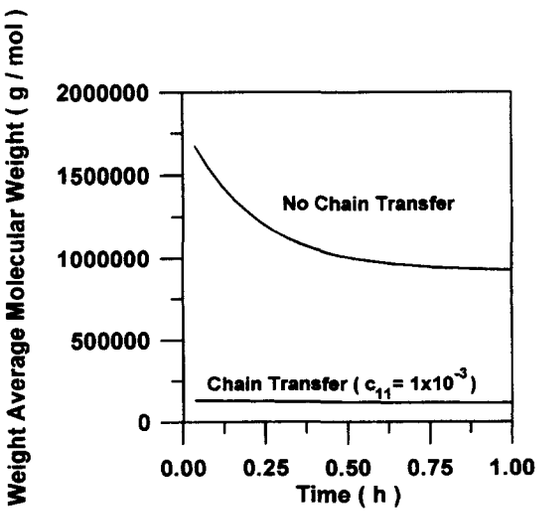

Figure 6 Weight average molecular weight for AA homopolymerization in ETOH. ($M_{10} = 4.33\,\text{gmol}\,l^{-1}$, $ci_0 = 0.0095\,\text{gmol}\,l^{-1}$)

a precipitant solvent (which was water or ethyl acetate, depending on the polymer composition) by centrifugation. Centrifugations were carried out for 10–15 min at 5000 rpm with a Janetzki centrifuge. Molecular weights of copolymers and homopolymers of AA and VA were evaluated by g.p.c. in different solvents, according to the copolymer composition (THF for VA homopolymers, water for AA homopolymers and DMF for AA/VA copolymers). Monodisperse polymers were used as calibrating standards.

MODELLING

A classical free-radical copolymerization mechanism[13] is used here to describe the AA/VA copolymerization in ETOH. The kinetic mechanism and model equations are presented in detail in the Appendix.

The mathematical model presented depends on the following parameters: k_d, r_1, r_2, K_1, K_2, ϕ_{12}, c_{11}, c_{12}, c_{21}, c_{22}, and f. The first three parameters are available in the literature. The kinetic constant of initiator decomposition is equal to[14]

$$k_d = 1.7215 \times 10^{15} e^{(-15924/T)} \quad (1)$$

while the reactivity ratios are equal to $r_1 = 2.6$ and $r_2 = 0.04$[4], where 1 refers to AA and 2 refers to VA. The other parameters are estimated, based on batch polymerization data. AA batch homopolymerization conversion data is used to allow the estimation of K_1. VA batch homopolymerization conversion data is used to allow the estimation of K_2. AA/VA batch copolymerization conversion and polymer composition data are used to allow the estimation of ϕ_{12}. Molecular weight distribution data are used to allow the evaluation of c_{11}, c_{12}, c_{21} and c_{22}. f is assumed to be constant and equal to 0.6. It is important to notice that the model is not very sensitive to f in the way it was written. All parameters are estimated with a standard maximum likelihood estimation routine[15]. The mathematical model and the estimated parameters are then validated by comparing experimental and theoretical results obtained in continuous copolymerizations. The model is then used to design the operation conditions that are necessary to meet certain final polymer specifications.

RESULTS AND DISCUSSION

Figures 1–3 show results obtained for VA homopolymerization in ETOH. It may be seen that the model is able to fit the experimental data very well when K_2 is equal to 9.57 ± 1.36 $(1/\text{gmol h})^{1/2}$ and c_{22} is equal to 5.0×10^{-3}. The results obtained show that chain transfer should not be neglected during VA polymerization in

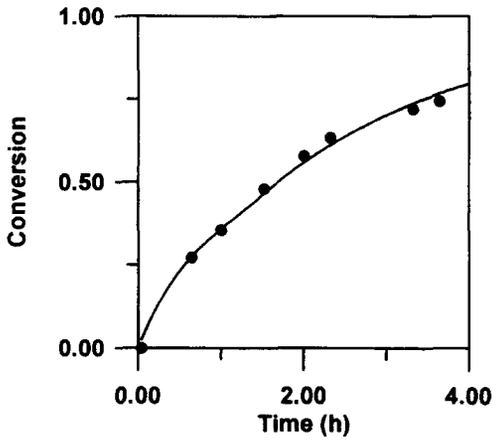

Figure 7 Monomer conversion for AA/VA copolymerization in ETOH. ($M_{10} = 0.58\,\text{gmol}\,l^{-1}$, $M_{20} = 2.81\,\text{gmol}\,l^{-1}$, $ci_0 = 0.0125\,\text{gmol}\,l^{-1}$)

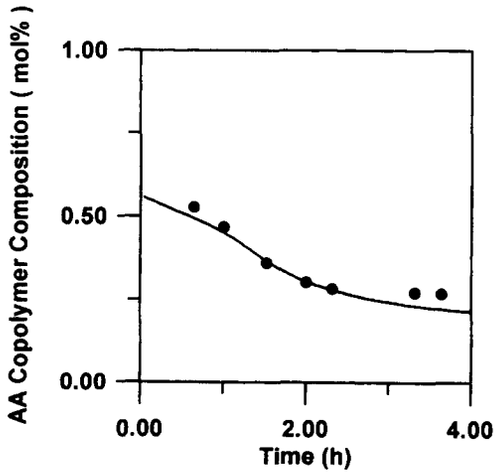

Figure 8 Copolymer composition for AA/VA copolymerization in ETOH. ($M_{10} = 0.58\,\text{gmol}\,l^{-1}$, $M_{20} = 2.81\,\text{gmol}\,l^{-1}$, $ci_0 = 0.0125\,\text{gmol}\,l^{-1}$)

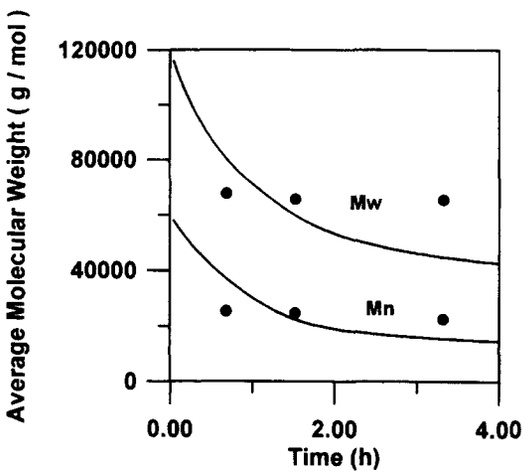

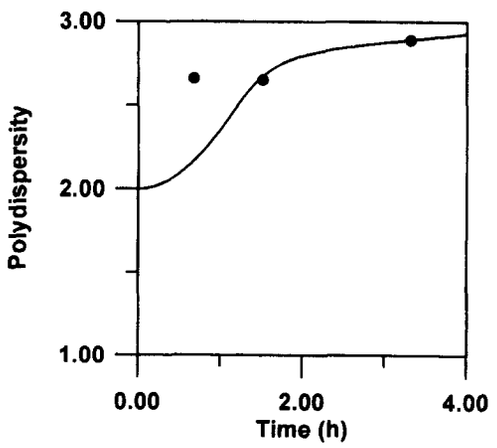

Figure 9 Average molecular weight for AA/VA copolymerization in ETOH. ($M_{10} = 0.58\,\text{gmol}\,l^{-1}$, $M_{20} = 2.81\,\text{gmol}\,l^{-1}$, $ci_0 = 0.0125\,\text{gmol}\,l^{-1}$)

ETOH; otherwise, average molecular weights are over-predicted by the model. These results are very similar to results presented by Brandrup and Immergut[16] for VA homopolymerization in other solvents ($8 < K_2 < 15\,h^{-1}$ and $1.0 \times 10^{-4} < c_{22} < 3.0 \times 10^{-3}$), showing that experimental and theoretical results are consistent. One point that must be noticed, though, is that chain transfer is likely to occur for both monomer and solvent molecules. However, it is not intended here to provide individual chain transfer constants for all chemical species present in the polymerization medium, but to show that chain transfer controls the molecular weight distribution.

Figures 4–6 show results obtained for AA homopolymerization in ETOH. It may be seen that the model is able to fit experimental conversion data when K_1 is equal to 117.2 ± 16.8 $(l/gmol\,h)^{1/2}$. Experimental molecular weight data obtained indicate that average molecular weights are well above $4 \times 10^5\,g\,gmol^{-1}$. However, these data could not be used for model building because the values obtained were larger than the average molecular weights of the samples available to calibrate the g.p.c. In spite of that, *Figures 5* and *6* show that chain transfer can probably be neglected during AA polymerization in ETOH because average molecular weights are very sensitive to small changes of the chain transfer constant. For instance, when c_{11} is equal to 1×10^{-3}, average molecular weights are around $50\,000\,g\,gmol^{-1}$, which are much lower than the values observed. Therefore, it may be said that chain transfer of AA radicals to AA and ETOH molecules is not significant, specially when compared to values observed for VA polymerizations. These results are very similar to results presented by Brandrup and Immergut[16] for AA homopolymerization in other solvents ($25 < K_1 < 250\,h^{-1}$ and $1.0 \times 10^{-5} < c_{11} < 1.0 \times 10^{-4}$), showing that experimental and theoretical results are consistent.

AA/VA copolymerizations were then carried out in order to allow the estimation of the cross-termination constant, based on both monomer conversion and

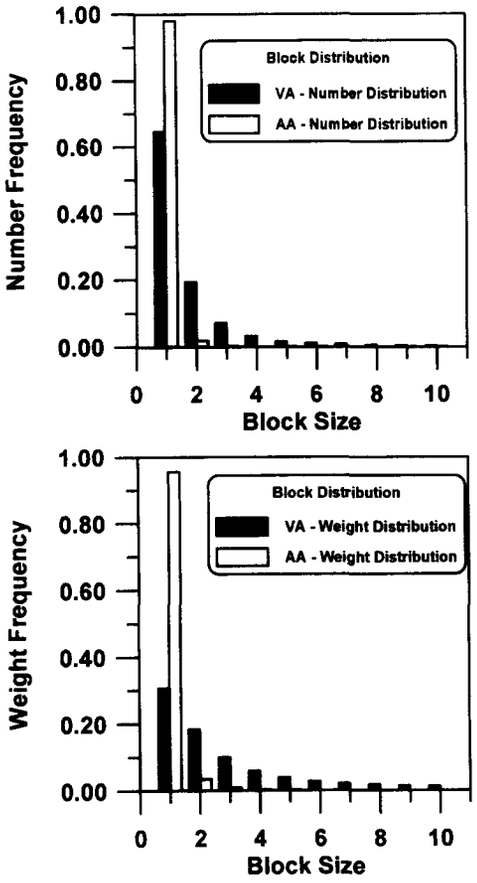

Figure 10 Block size distributions for AA/VA copolymerization in ETOH. ($M_{10} = 0.58\,gmol\,l^{-1}$, $M_{20} = 2.81\,gmol\,l^{-1}$, $ci_0 = 0.0125\,gmol\,l^{-1}$)

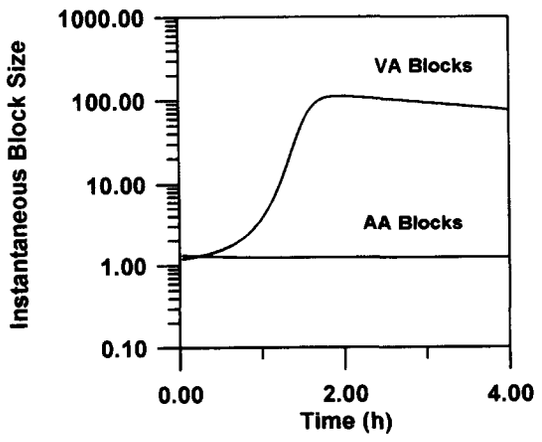

Figure 11 Instantaneous number average block sizes for AA/VA copolymerization in ETOH. ($M_{10} = 0.58\,gmol\,l^{-1}$, $M_{20} = 2.81\,gmol\,l^{-1}$, $ci_0 = 0.0125\,gmol\,l^{-1}$)

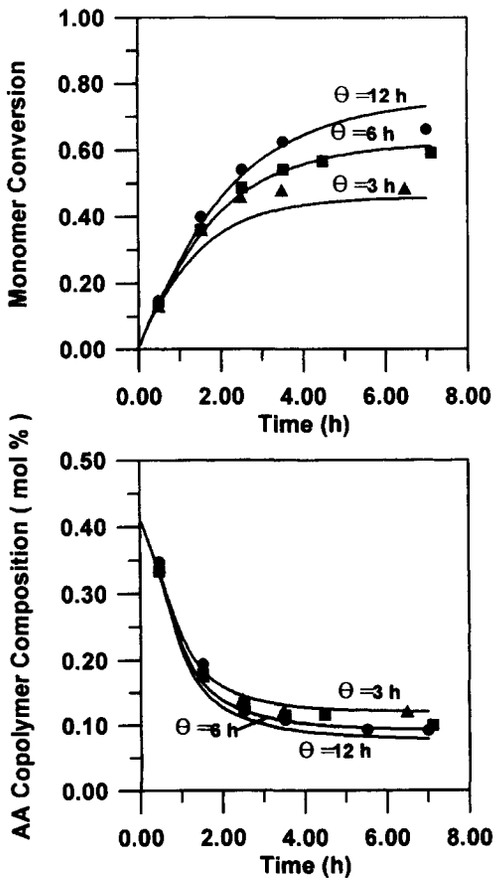

Figure 12 Monomer conversion and copolymer composition for continuous AA/VA copolymerization in ETOH. [$M_{1f} = 0.193\,gmol\,l^{-1}$, $M_{2f} = 3.10\,gmol\,l^{-1}$, $ci_f = 0.0104\,gmol\,l^{-1}$. $\Theta = 3\,h$ (▲), $\Theta = 6\,h$ (■), $\Theta = 12\,h$ (●)]

copolymer composition data. Results obtained when ϕ_{12} is equal to 27.15 ± 4.54 are presented in *Figures 7* and *8*. It may be seen that experimental and theoretical results agree very well. To our knowledge, values of ϕ_{12} for AA/VA copolymerizations are not available in the literature for comparison. However, ϕ_{12} is usually in the range $1 < \phi_{12} < 300$, so that the estimated value is reasonable when compared to values obtained for other copolymerization systems. *Figure 9* presents molecular weight data obtained when chain transfer of VA radicals to VA molecules is assumed to control the molecular weight distribution, as observed previously. Results may be regarded as good, although observed data showed smaller variations than simulation results during the batch. Therefore, it is assumed from now on that all chain transfer constants are equal to zero, except c_{11}, which is equal to 5.0×10^{-3} and controls the molecular weight of the copolymer.

Figures 10 and *11* show block frequency distribution data, as predicted by the model. It may be observed that, at the conditions analysed, blocks are small, in spite of the very different reactivity ratios. This means that it is possible to produce relatively homogeneous polymer chains, in spite of the very different reactivity ratios, which favour the consumption of AA molecules. *Figure 11* shows that the instantaneous average AA block size is roughly the same along the whole batch, while instantaneous average VA block size grows continuously along the batch, so that VA homopolymer is produced at the end of the batch. This occurs because AA is consumed at faster rates than VA, which also causes the composition drift presented in *Figure 8*.

In order to validate the model and allow the production of polymer chains with uniform composition, several experiments were carried out in continuous stirred tank reactors, with different feed compositions and at different residence times. Results are presented in *Figures 12–14*. Both experimental and theoretical results were obtained by charging the reactor with the feed mixture at 75°C and monitoring monomer conversion and copolymer composition until reaching steady state conditions. An experimental technique has been recently developed to allow the in-line monitoring of both monomer conversion and copolymer composition in such reactors[17]. In all cases, agreement between experimental and theoretical results is very good, which shows the adequacy of the parameters estimated previously. The fractionation of the copolymer produced at continuous operation showed that the composition of the copolymer chains is uniform, as expected. Fractionation results are presented in *Figures 15* and *16*, where it may be seen that fluctuations around average composition values are very small for both VA rich and AA rich copolymers.

As copolymer with uniform composition can be produced at continuous reactors and as the model is able to reproduce experimental data, simulations were carried out to map the operation conditions that can allow the production of copolymer with specified composition with small average AA block sizes, for

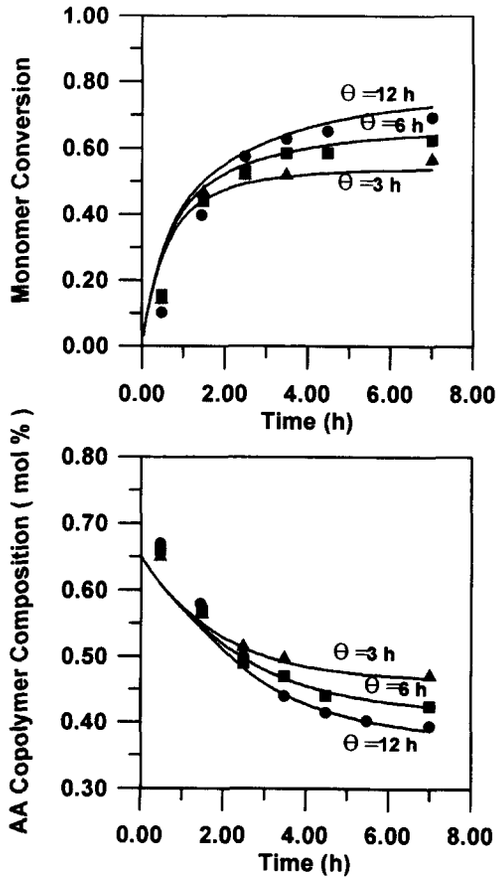

Figure 13 Monomer conversion and copolymer composition for continuous AA/VA copolymerization in ETOH. [$M_{1f} = 1.011\,\text{gmol}\,l^{-1}$, $M_{2f} = 2.487\,\text{gmol}\,l^{-1}$, $ci_f = 0.0107\,\text{gmol}\,l^{-1}$. Θ = 3 h (▲), Θ = 6 h (■), Θ = 12 h (●)]

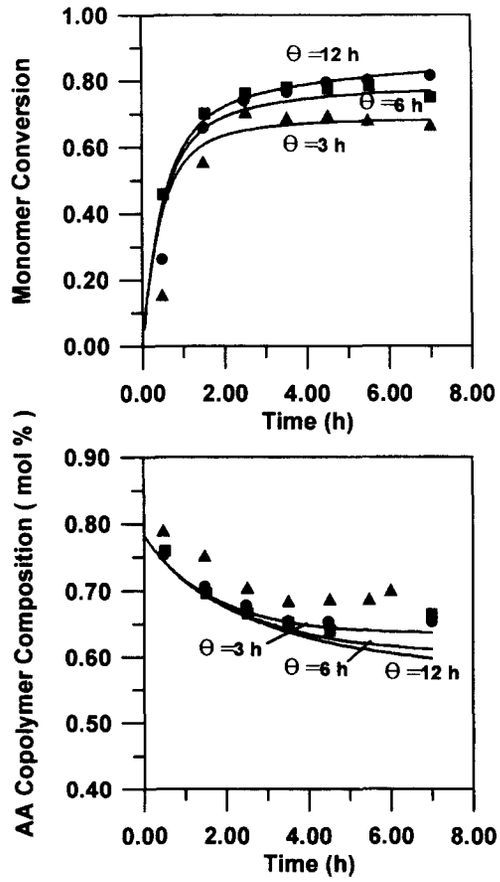

Figure 14 Monomer conversion and copolymer composition for continuous AA/VA copolymerization in ETOH [$M_{1f} = 1.929\,\text{gmol}\,l^{-1}$, $M_{2f} = 1.803\,\text{gmol}\,l^{-1}$, $ci_f = 0.0109\,\text{gmol}\,l^{-1}$. Θ = 3 h (▲), Θ = 6 h (■), Θ = 12 h (●)]

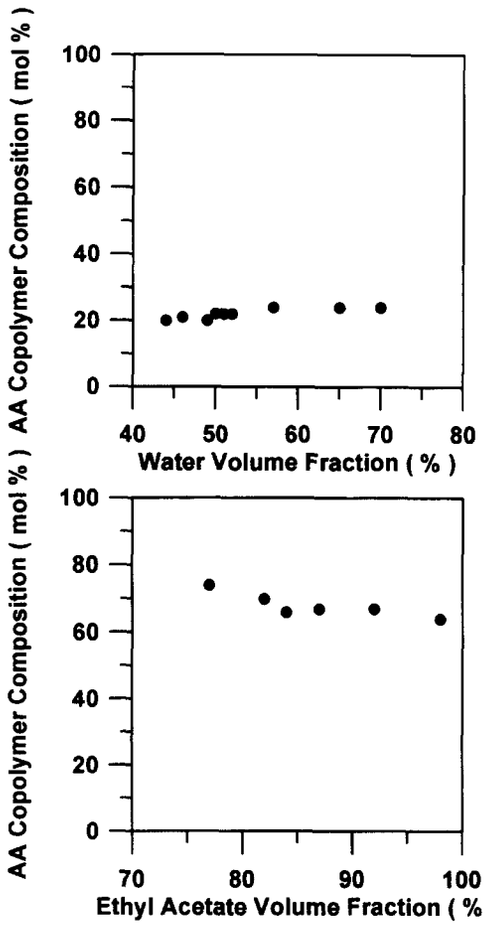

Figure 15 Copolymer composition of copolymer fractions in continuous reactions—copolymers with 22 and 66 mol% of AA

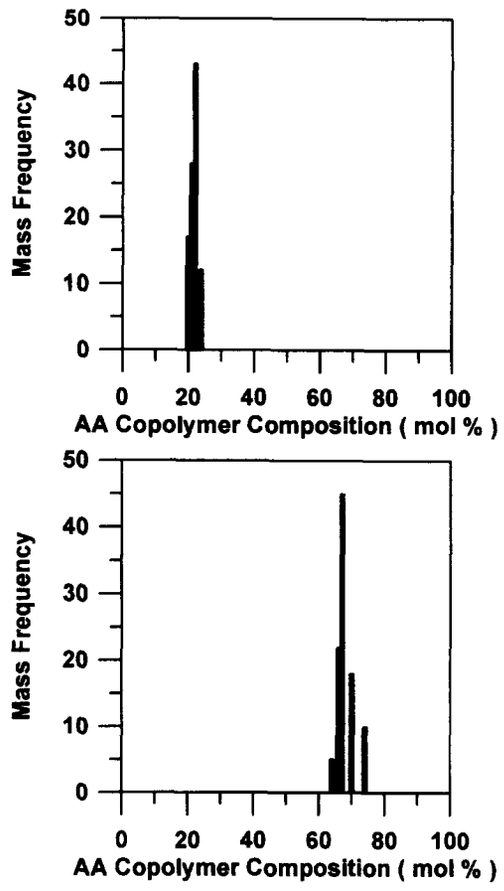

Figure 16 Copolymer composition distributions in continuous reactions—copolymers with 22 and 66 mol% of AA

certain applications. Results are summarized in *Figures 17–20*. *Figure 17* shows that, if AA blocks are to be avoided, AA copolymer composition cannot be greater than 65 mol%. *Figures 18* and *19* show how monomer conversion and normalized polymer productivity, defined as

$$x = \frac{M_{1f} + M_{2f} - M_1 - M_2}{M_{1f} + M_{2f}} \tag{2}$$

$$\text{xprod} = \frac{x}{\Theta} \tag{3}$$

respond to variations of the desired copolymer composition and of the residence time. It can be seen that the sensitivity to changes of the desired copolymer composition is not very significant at low AA contents, as VA consumption rate is the slowest one and controls the reaction process. It can also be seen that both monomer conversion and polymer productivity are small at the conditions analysed, so that more detailed optimization studies must be carried out in order to improve process operation. *Figure 20* shows the normalized feed concentrations needed to produce the specified copolymer, as a function of residence time. The normalized feed composition is defined as

$$f_{\text{norm}} = \frac{1 - x_1}{(M_{2f}/M_{1f}) + 1} \tag{4}$$

where x_1 is the desired AA conversion. As the ratio M_{2f}/M_{1f} must be positive, it can be shown that the maximum allowed specified AA conversion is $1 - f_{\text{norm}}$.

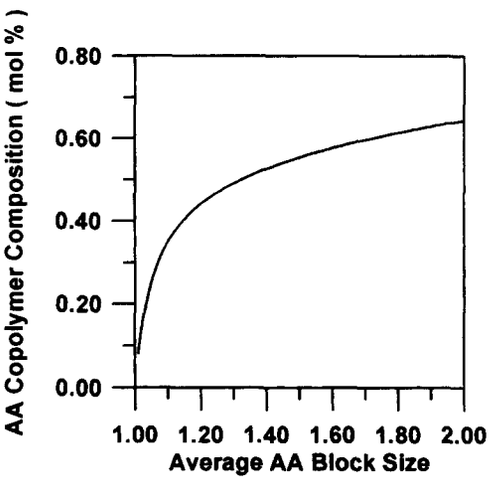

Figure 17 Correlation between copolymer composition and average AA block size—model predictions. ($M_{1f} = 0.58\,\text{gmol}\,l^{-1}$, $M_{2f} = 2.81\,\text{gmol}\,l^{-1}$, $ci_f = 0.0125\,\text{gmol}\,l^{-1}$)

As it can be seen, at the conditions analysed AA conversions above 99% can only be obtained if the AA copolymer composition is below 30 mol%, although AA conversions above 90% can be obtained in the whole range of AA compositions of interest.

CONCLUSIONS

A model was developed to describe the AA/VA copolymerization in batch and continuous stirred tank reactors. Batch experiments were then carried out

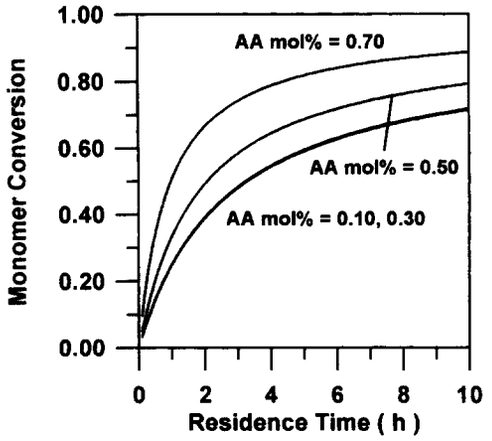

Figure 18 Correlation between monomer conversion and residence time for different specified copolymer compositions—model predictions. ($M_{1f} = 0.58\,\text{gmol}\,l^{-1}$, $M_{2f} = 2.81\,\text{gmol}\,l^{-1}$, $ci_f = 0.0125\,\text{gmol}\,l^{-1}$)

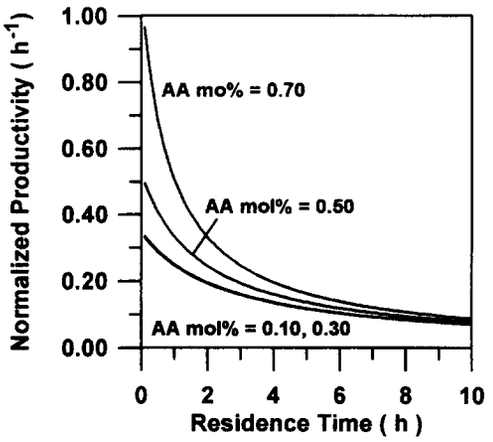

Figure 19 Correlation between polymer productivity and residence time for different specified copolymer compositions—model predictions. ($M_{1f} = 0.58\,\text{gmol}\,l^{-1}$, $M_{2f} = 2.81\,\text{gmol}\,l^{-1}$, $ci_f = 0.0125\,\text{gmol}\,l^{-1}$)

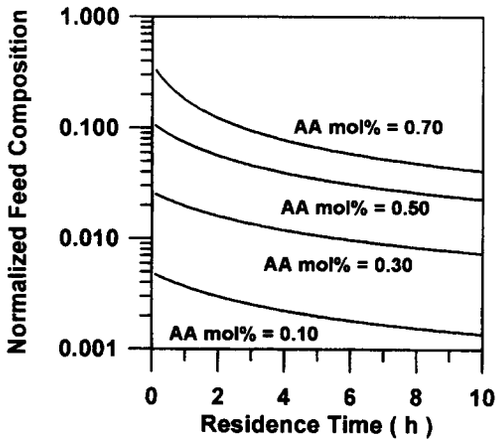

Figure 20 Correlation between feed conditions and residence time for different specified copolymer compositions—model predictions. ($M_{1f} = 0.58\,\text{gmol}\,l^{-1}$, $M_{2f} = 2.81\,\text{gmol}\,l^{-1}$, $ci_f = 0.0125\,\text{gmol}\,l^{-1}$)

to allow the estimation of lacking copolymerization parameters, which allowed excellent fittings of monomer conversion and copolymer composition data and showed that molecular weight distributions are controlled by chain transfer of VA terminated radicals. Experiments were then carried out in continuous reactors to validate the model and it was shown that model predictions were very good in all conditions analysed. The model was then used to show that AA/VA copolymers with uniform composition can be produced in continuous reactors with small average AA block sizes, if AA copolymer compositions are smaller than 65 mol%.

REFERENCES

1. Mark, H. F., Bikales, N. M. and Overberger, C. G., *Encyclopedia of Polymer Science and Engineering*, Vol. 10. Wiley Interscience, New York, 1987, p. 222.
2. Brar, A. S. and Sunita, *Eur. Polym. J.*, 1991, **27** (1), 17.
3. Bourdais, J., *Bull. Soc. Chim. France*, 1955, 485.
4. Zaldívar, C., Iglesias, G. and del Sol, O., Submitted to *Polymer*, 1996.
5. Heublein, B., Heublein, G., Marschner, H., Krahnert, L. and Mey, E. M., *VEB Chemische Werke Buna, Ger. (East)*, DD 222885 ClC08F218/08, 29 May 1985, Appl. 261, 847, 11 Apr. 1984, 8 pp.
6. Heublein, B., Hotzel, H. and Schultz, H., *Acta Polym.*, 1985, **38** (4), 234.
7. Heublein, B., Schultz, H. and Heublein, G., *Acta Polym.*, 1987, **38** (2), 150.
8. Heublein, B., Burckhardt, A. and Heublein, G., *Acta Polym.*, 1988, **39** (3), 136.
9. Heublein, B. and Heublein, G., *Acta Polym.*, 1988, **39** (6), 324.
10. Heublein, B. and Heublein, G., *Acta Polym.*, 1988, **39** (6), 326.
11. Zaldívar, C. and Iglesias, G., Internal Report, CNIC, Habana, 1995.
12. Zaldívar, C., Iglesias, G., Suzarte, A. and Pinto, J. C., Submitted to *Polymer*, 1996.
13. Odian, G., *Principles of Polymerization*, 3rd edn. Wiley, New York, 1991.
14. Fontoura, J. M. R., Controle de um Reator de Polimerização Descontínuo. M.Sc. thesis, PEQ/COPPE/UFRJ, Rio de Janeiro (in Portuguese), 1996.
15. Noronha, F. B., Pinto, J. C., Monteiro, J. L., Lobão, M. W. and Santos, T. J., ESTIMA—Um Pacote Computacional para Estimação de Parâmetros e Projeto de Experimentos, Internal Report, PEQ/COPPE/UFRJ, Rio de Janeiro (in Portuguese), 1993.
16. Brandrup, J. and Immergut, E. H., *Polymer Handbook*, 3rd edn. Wiley, New York, 1989.
17. Zaldívar, C., Iglesias, G., del Sol, O. and Pinto, J. C., Submitted to *Polymer*, 1996.
18. Ray, W. H., *J. Macromol. Sci.-Revs. Macrom. Chem.*, 1972, **C8**, 1.

NOMENCLATURE

c_{ij}	ratio between k_{trij} and k_{pij}
f	initiator efficiency
f	ratio between M_1 and M_2
f_{norm}	normalized feed composition
F	function defined by equation (A47)
$\bar{i}$	average block size
I	initiator
k_d	kinetic constant for initiator decomposition
k_{pij}	kinetic constant for propagation of radical i with monomer j
k_{tij}	kinetic constant for termination of radical i with radical j
k_{trij}	kinetic constant for chain transfer of radical i to monomer j
K_i	kinetic parameters defined by equations (A5)–(A6)
M_i	monomer i
$P_{i,j}$	radical chain containing i mers of species 1 and j mers of species 2 in the chain and the species 1 at the active site (radical 1)

PD polydispersity
PM_n number average polymer molecular weight
PM_w weight average polymer molecular weight
q_i propagation probability defined by equations (A28)–(A29)
$Q_{i,j}$ radical chain containing i mers of species 1 and j mers of species 2 in the chain and the species 2 at the active site (radical 2)
r_i reactivity ratio
R radical fragment
s_i radical blocks containing i mers of species 2
S_i dead blocks containing i mers of species 2
t time
t_i radical blocks containing i mers of species 1
T_i dead blocks containing i mers of species 1
x total monomer conversion
x_1 molar fraction of species 1 in the polymer chains
x_{prod} normalized polymer productivity

Greek

ϕ_i moments of the radical 2 block size distribution
Φ_i moments of the dead block size distribution of species 2
ϕ_{12} cross termination constant
$\lambda_{i,j}$ moments of the radical 1 chain size distribution
$\Lambda_{i,j}$ dead polymer chain containing i mers of species 1 and j mers of species 2
$\mu_{i,j}$ moments of the dead polymer chain size distribution
π_i moments of the radical 1 block size distribution
Π_i moments of the dead block size distribution of species 1
θ residence time
$\xi_{i,j}$ moments of the radical 2 chain size distribution

Special subscripts

1 acrylic acid
2 vinyl acetate
f feed

APPENDIX: KINETIC MECHANISM AND MODEL EQUATIONS

The kinetic mechanism comprises the following steps:

Initiation

$$I \xrightarrow{k_d} 2R$$

$$R + M_1 \xrightarrow{k_1} P_{1,0}$$

$$R + M_2 \xrightarrow{k_2} Q_{0,1}$$

Propagation

$$P_{i,j} + M_1 \xrightarrow{k_{p11}} P_{i+1,j}$$

$$P_{i,j} + M_2 \xrightarrow{k_{p12}} Q_{i,j+1}$$

$$Q_{i,j} + M_1 \xrightarrow{k_{p21}} P_{i+1,j}$$

$$Q_{i,j} + M_2 \xrightarrow{k_{p22}} Q_{i,j+1}$$

Transfer to monomer

$$P_{i,j} + M_1 \xrightarrow{k_{tr11}} \Lambda_{i,j} + P_{1,0}$$

$$P_{i,j} + M_2 \xrightarrow{k_{tr12}} \Lambda_{i,j} + Q_{0,1}$$

$$Q_{i,j} + M_1 \xrightarrow{k_{tr21}} \Lambda_{i,j} + P_{1,0}$$

$$Q_{i,j} + M_2 \xrightarrow{k_{tr22}} \Lambda_{i,j} + Q_{0,1}$$

Termination by disproportionation

$$P_{i,j} + P_{m,n} \xrightarrow{k_{t22}} \Lambda_{i,j} + \Lambda_{m,n}$$

$$P_{i,j} + Q_{m,n} \xrightarrow{k_{t22}} \Lambda_{i,j} + \Lambda_{m,n}$$

$$Q_{i,j} + Q_{m,n} \xrightarrow{k_{t22}} \Lambda_{i,j} + \Lambda_{m,n}$$

If the reactor volume is constant and the quasi steady state and long chain assumptions for radicals are valid, then the following mass balance equations may be written

$$\frac{dI}{dt} = \frac{(I_f - I)}{\theta} - k_d I \tag{A1}$$

$$\frac{dM_1}{dt} = \frac{(M_{1f} - M_1)}{\theta} - k_{p11} P M_1 - k_{p21} Q M_1 = \frac{(M_{1f} - M_1)}{\theta} - (k_{p11} P)\left(M_1 - \frac{M_2}{r_1}\right) \tag{A2}$$

$$\frac{dM_2}{dt} = \frac{(M_{2f} - M_2)}{\theta} - k_{p12} P M_2 - k_{p22} Q M_2 = \frac{(M_{2f} - M_2)}{\theta} - (k_{p11} P)\left(\frac{M_2}{r_1} - \frac{r_2}{r_1}\frac{M_2^2}{M_1}\right) \tag{A3}$$

where

$$(k_{p11}P) = \sqrt{\frac{2k_d I}{\left(\frac{1}{K_1}\right)^2 + 2\phi_{12}\frac{1}{K_1}\frac{1}{K_2}\frac{M_2}{M_1}\frac{r_2}{r_1} + \left(\frac{1}{K_2}\frac{M_2}{M_1}\frac{r_2}{r_1}\right)^2}} \tag{A4}$$

$$K_1 = \sqrt{\frac{f k_{p11}^2}{k_{t11}}} \tag{A5}$$

$$K_2 = \sqrt{\frac{f k_{p22}^2}{k_{t22}}} \tag{A6}$$

r_1 and r_2 are the reactivity ratios and ϕ_{12} is the cross termination constant.

In order to describe the evolution of the molecular weight distribution (MWD), the method of moments is used. The statistical moments of the MWD are defined as[14]

$$\mu_{k,1} = \sum_{i=0}^{\infty}\sum_{j=0}^{\infty} i^k j^1 \Lambda_{i,j} \tag{A7}$$

$$\lambda_{k,1} = \sum_{i=1}^{\infty}\sum_{j=0}^{\infty} i^k j^1 P_{i,j} \tag{A8}$$

$$\xi_{k,1} = \sum_{i=0}^{\infty}\sum_{j=1}^{\infty} i^k j^1 Q_{i,j} \tag{A9}$$

so that

$$PM_n = \frac{\mu_{1,0} PM_1 + \mu_{0,1} PM_2}{\mu_{0,0}} \tag{A10}$$

$$PM_w = \frac{\mu_{2,0}PM_1^2 + \mu_{1,1}PM_1PM_2 + \mu_{0,2}PM_2^2}{\mu_{1,0}PM_1 + \mu_{0,1}PM_2} \quad \text{(A11)}$$

$$PD = \frac{PM_w}{PM_n} \quad \text{(A12)}$$

According to the kinetic mechanism:

$$\frac{d\mu_{k,1}}{dt} = (k_{p11}\lambda_{k,1})\left(c_{11}M_1 + \frac{c_{12}}{r_1}M_2 + \frac{f}{K_1^2}(k_{p11}P) + \phi_{12}f\frac{1}{K_1}\frac{1}{K_2}(k_{p22}Q)\right) + (k_{p22}\xi_{k,1})\left(\frac{c_{21}}{r_2}M_1 + c_{22}M_2 + \phi_{12}f\frac{1}{K_1}\frac{1}{K_2}(k_{p11}P) + \frac{f}{K_2^2}(k_{p22}Q)\right) - \frac{\mu_{k,1}}{\theta} \quad \text{(A13)}$$

where

$$(kp_{11}\lambda_{0,0}) = (kp_{11}P) \quad \text{(A14)}$$

$$(kp_{22}\xi_{0,0}) = \frac{M_2r_2}{M_1r_1}(kp_{11}P) \quad \text{(A15)}$$

$(k_{p11}\lambda_{1,0})$ and $(k_{p22}\xi_{1,0})$are the solutions of

$$\left[\frac{M_2}{r_1} + c_{11}M_1 + \frac{c_{12}}{r_1}M_2 + \frac{f}{K_1^2}(kp_{11}\lambda_{0,0}) + \phi_{12}f\frac{1}{K_1}\frac{1}{K_2}(k_{p22}\xi_{0,0})\right](k_{p11}\lambda_{1,0}) - \frac{M_1}{r_2}(k_{p22}\xi_{1,0}) = (2fk_dI)\frac{M_1}{M_1+M_2} + \frac{M_1}{r_2}(1+c_{21})(k_{p22}\xi_{0,0}) + M_1(1+c_{11})(kp_{11}\lambda_{0,0}) \quad \text{(A16)}$$

$$-\frac{M_2}{r_1}(k_{p11}\lambda_{1,0}) + \left[\frac{M_1}{r_2} + \frac{c_{21}}{r_2}M_1 + c_{22}M_2 + \frac{f}{K_2^2}(k_{p22}\xi_{0,0}) + \phi_{12}f\frac{1}{K_1}\frac{1}{K_2}(k_{p11}\lambda_{0,0})\right](k_{p22}\xi_{1,0}) = 0 \quad \text{(A17)}$$

$(k_{p11}\lambda_{0,1})$ and $(k_{p22}\xi_{0,1})$ are the solutions of

$$\left[\frac{M_2}{r_1} + c_{11}M_1 + \frac{c_{12}}{r_1}M_2 + \frac{f}{K_1^2}(kp_{11}\lambda_{0,0}) + \phi_{12}f\frac{1}{K_1}\frac{1}{K_2}(k_{p22}\xi_{0,0})\right](k_{p11}\lambda_{0,1}) - \frac{M_1}{r_2}(k_{p22}\xi_{0,1}) = 0 \quad \text{(A18)}$$

$$-\frac{M_2}{r_1}(k_{p11}\lambda_{0,1}) + \left[\frac{M_1}{r_2} + \frac{c_{21}}{r_2}M_1 + c_{22}M_2 + \frac{f}{K_2^2}(k_{p22}\xi_{0,0}) + \phi_{12}f\frac{1}{K_1}\frac{1}{K_2}(k_{p11}\lambda_{0,0})\right](k_{p22}\xi_{0,1}) = (2fk_dI)\frac{M_2}{M_1+M_2} + \frac{M_2}{r_1}(1+c_{12})(k_{p11}\lambda_{0,0}) + M_2(1+c_{22})(kp_{22}\xi_{0,0}) \quad \text{(A19)}$$

$(k_{p11}\lambda_{2,0})$ and $(k_{p22}\xi_{2,0})$ are the solutions of

$$\left[\frac{M_2}{r_1} + c_{11}M_1 + \frac{c_{12}}{r_1}M_2 + \frac{f}{K_1^2}(kp_{11}\lambda_{0,0}) + \phi_{12}f\frac{1}{K_1}\frac{1}{K_2}(k_{p22}\xi_{0,0})\right](k_{p11}\lambda_{2,0}) - \frac{M_1}{r_2}(k_{p22}\xi_{2,0}) = (2fk_dI)\frac{M_1}{M_1+M_2} + \frac{M_1}{r_2}(1+c_{21})(k_{p22}\xi_{0,0}) + M_1(1+c_{11})(kp_{11}\lambda_{0,0}) + 2M_1(k_{p11}\lambda_{1,0}) + 2\frac{M_1}{r_2}(k_{p22}\xi_{1,0}) \quad \text{(A20)}$$

$$-\frac{M_2}{r_1}(k_{p11}\lambda_{2,0}) + \left[\frac{M_1}{r_2} + \frac{c_{21}}{r_2}M_1 + c_{22}M_2 + \frac{f}{K_2^2}(k_{p22}\xi_{0,0}) + \phi_{12}f\frac{1}{K_1}\frac{1}{K_2}(k_{p11}\lambda_{0,0})\right](k_{p22}\xi_{2,0}) = 0 \quad \text{(A21)}$$

$(k_{p11}\lambda_{0,2})$ and $(k_{p22}\xi_{0,2})$ are the solutions of

$$\left[\frac{M_2}{r_1} + c_{11}M_1 + \frac{c_{12}}{r_1}M_2 + \frac{f}{K_1^2}(kp_{11}\lambda_{0,0}) + \phi_{12}f\frac{1}{K_1}\frac{1}{K_2}(k_{p22}\xi_{0,0})\right](k_{p11}\lambda_{0,2}) - \frac{M_1}{r_2}(k_{p22}\xi_{0,2}) = 0 \quad \text{(A22)}$$

$$-\frac{M_2}{r_1}(k_{p11}\lambda_{0,2}) + \left[\frac{M_1}{r_2} + \frac{c_{21}}{r_2}M_1 + c_{22}M_2 + \frac{f}{K_2^2}(k_{p22}\xi_{0,0}) + \phi_{12}f\frac{1}{K_1}\frac{1}{K_2}(k_{p11}\lambda_{0,0})\right](k_{p22}\xi_{0,2}) = (2fk_dI)\frac{M_2}{M_1+M_2} + \frac{M_2}{r_1}(1+c_{12})(k_{p11}\lambda_{0,0}) + M_2(1+c_{22})(kp_{22}\xi_{0,0}) + 2\frac{M_2}{r_1}(k_{p11}\lambda_{0,1}) + 2M_2(fkp_{22}\xi_{0,1}) \quad \text{(A23)}$$

$(k_{p11}\lambda_{1,1})$ and $(k_{p22}\xi_{1,1})$ are the solutions of

$$\left[\frac{M_2}{r_1} + c_{11}M_1 + \frac{c_{12}}{r_1}M_2 + \frac{f}{K_1^2}(kp_{11}\lambda_{0,0}) + \phi_{12}f\frac{1}{K_1}\frac{1}{K_2}(k_{p22}\xi_{0,0})\right](k_{p11}\lambda_{1,1}) - \frac{M_1}{r_2}(k_{p22}\xi_{1,1}) = \frac{M_1}{r_2}(k_{p22}\xi_{0,1}) + M_1(kp_{11}\lambda_{0,1}) \quad \text{(A24)}$$

$$-\frac{M_2}{r_1}(k_{p11}\lambda_{1,1}) + \left[\frac{M_1}{r_2} + \frac{c_{21}}{r_2}M_1 + c_{22}M_2 + \frac{f}{K_2^2}(k_{p22}\xi_{0,0}) + \phi_{12}f\frac{1}{K_1}\frac{1}{K_2}(k_{p11}\lambda_{0,0})\right](k_{p22}\xi_{1,1}) = \frac{M_2}{r_1}(k_{p11}\lambda_{1,0}) + M_2(kp_{22}\xi_{1,0}) \quad \text{(A25)}$$

The kinetic mechanism can also be rewritten in order to allow the computation of block size distributions in

the final polymer chains. In this case, it is convenient to write:

Initiation

$$I \xrightarrow{k_d} 2R$$

$$R + M_1 \xrightarrow{k_1} t_1$$

$$R + M_2 \xrightarrow{k_2} s_1$$

Propagation

$$t_i + M_1 \xrightarrow{k_{p11}} t_{i+1}$$

$$t_i + M_2 \xrightarrow{k_{p12}} T_i + s_1$$

$$s_i + M_1 \xrightarrow{k_{p21}} S_i + t_1$$

$$s_i + M_2 \xrightarrow{k_{p22}} s_{i+1}$$

Chain transfer to monomer

$$t_i + M_1 \xrightarrow{k_{tr11}} T_i + t_1$$

$$t_i + M_2 \xrightarrow{k_{tr12}} T_i + s_1$$

$$s_i + M_1 \xrightarrow{k_{tr21}} S_i + t_1$$

$$s_i + M_2 \xrightarrow{k_{tr22}} S_i + s_1$$

Termination by disproportionation

$$t_i + t_j \xrightarrow{k_{t22}} T_i + T_j$$

$$t_i + s_j \xrightarrow{k_{t22}} T_i + S_j$$

$$s_i + s_j \xrightarrow{k_{t22}} S_i + S_j$$

Then, the following equations can be written

$$\frac{dT_i}{dt} = \left[\frac{M_2}{r_1} + c_{11}M_1 + \frac{c_{12}}{r_1}M_2 + \frac{f}{K_1^2}(k_{p11}\lambda_{0,0}) + \phi_{12}f\frac{1}{K_1}\frac{1}{K_2}(k_{p22}\xi_{0,0})\right] \times \left[\frac{2fk_dI}{M_1+M_2} + \frac{(k_{p22}\xi_{0,0})}{r_2} + c_{11}(k_{p11}\lambda_{0,0}) + \frac{c_{21}}{r_2}(k_{p22}\xi_{0,0})\right]q_1^i - \frac{T_i}{\theta} \quad \text{(A26)}$$

$$\frac{dS_i}{dt} = \left[\frac{M_1}{r_2} + c_{22}M_2 + \frac{c_{21}}{r_2}M_1 + \frac{f}{K_2^2}(k_{p22}\xi_{0,0}) + \phi_{12}f\frac{1}{K_1}\frac{1}{K_2}(k_{p11}\lambda_{0,0})\right] \times \left[\frac{2fk_dI}{M_1+M_2} + \frac{(k_{p11}\lambda_{0,0})}{r_1} + c_{22}(k_{p22}\xi_{0,0}) + \frac{c_{12}}{r_1}(k_{p11}\lambda_{0,0})\right]q_2^i - \frac{S_i}{\theta} \quad \text{(A27)}$$

where

$$q_1 = \left\{M_1 \Big/ \left[M_1(1+c_{11}) + \frac{M_2}{r_1}(1+c_{12}) + \frac{f}{K_1^2}(k_{p11}\lambda_{0,0}) + \phi_{12}f\frac{1}{K_1}\frac{1}{K_2}(k_{p22}\xi_{0,0})\right]\right\} \quad \text{(A28)}$$

$$q_2 = \left\{M_2 \Big/ \left[M_2(1+c_{22}) + \frac{M_1}{r_2}(1+c_{21}) + \frac{f}{K_2^2}(k_{p22}\xi_{0,0}) + \phi_{12}f\frac{1}{K_1}\frac{1}{K_2}(k_{p11}\lambda_{0,0})\right]\right\} \quad \text{(A29)}$$

Equations (A26) and (A27) may be integrated in this form. As block sizes are usually much smaller than chain sizes, the number of equations necessary to describe the block size distribution does not need to be large. Equations (A26) and (A27) can also be averaged to allow the computation of the statistical moments of the block size distribution, as follows

$$\Pi_k = \sum_{i=1}^{\infty} i^k T_i \quad \text{(A30)}$$

$$\pi_k = \sum_{i=1}^{\infty} i^k t_i \quad \text{(A31)}$$

$$\Phi_k = \sum_{i=1}^{\infty} i^k S_i \quad \text{(A32)}$$

$$\phi_k = \sum_{i=1}^{\infty} i^k s_i \quad \text{(A33)}$$

$$\frac{d\Pi_k}{dt} = \left[\frac{M_2}{r_1} + c_{11}M_1 + \frac{c_{12}}{r_1}M_2 + \frac{f}{K_1^2}(k_{p11}\lambda_{0,0}) + \phi_{12}f\frac{1}{K_1}\frac{1}{K_2}(k_{p22}\xi_{0,0})\right](k_{p11}\pi_k) - \frac{\Pi_k}{\theta} \quad \text{(A34)}$$

$$\frac{d\Phi_k}{dt} = \left[\frac{M_1}{r_2} + c_{22}M_2 + \frac{c_{21}}{r_2}M_1 + \frac{f}{K_2^2}(k_{p22}\xi_{0,0}) + \phi_{12}f\frac{1}{K_1}\frac{1}{K_2}(k_{p11}\lambda_{0,0})\right](k_{p22}\phi_k) - \frac{\Phi_k}{\theta} \quad \text{(A35)}$$

$$(k_{p11}\pi_o) = (k_{p11}P) \quad \text{(A36)}$$

$$(k_{p11}\pi_1) = \left[\frac{2fk_dI}{M_1+M_2} + (1+c_{21})\frac{(k_{p22}\xi_{0,0})}{r_2} + (1+c_{11})(k_{p11}\lambda_{0,0})\right]q_1 \quad \text{(A37)}$$

$$(k_{p11}\pi_2) = \left[\frac{2fk_dI}{M_1+M_2} + (1+c_{21})\frac{(k_{p22}\xi_{0,0})}{r_2} + (1+c_{11})(k_{p11}\lambda_{0,0}) + 2(k_{p11}\pi_1)\right]q_1 \quad \text{(A38)}$$

$$(k_{p22}\phi_0) = (k_{p22}Q) \quad \text{(A39)}$$

$$(k_{p22}\phi_1) = \left[\frac{2fk_dI}{M_1+M_2} + (1+c_{12})\frac{(k_{p11}\lambda_{0,0})}{r_1} + (1+c_{22})(k_{p22}\xi_{0,0})\right]q_2 \quad \text{(A40)}$$

$$(k_{p22}\phi_2) = \left[\frac{2fk_dI}{M_1+M_2} + (1+c_{12})\frac{(k_{p11}\lambda_{0,0})}{r_1} + (1+c_{22})(k_{p22}\xi_{0,0}) + 2(k_{p22}\phi_1)\right]q_2 \quad \text{(A41)}$$

For short periods of time or at steady state conditions, equations (A26)–(A29) lead to exponential distributions with average block sizes equal to:

$$\overline{i_T} = \frac{1}{1-q_1} = \left\{M_1 \Big/ \left[c_{11}M_1 + \frac{M_2}{r_1}(1+c_{12}) + \frac{f}{K_1^2}(k_{p11}\lambda_{0,0}) + \phi_{12}f\frac{1}{K}\frac{1}{K_2}(k_{p22}\xi_{0,0})\right]\right\} + 1 \quad \text{(A42)}$$

$$\overline{i_S} = \frac{1}{1-q_2} = \left\{M_2 \Big/ \left[c_{22}M_2 + \frac{M_1}{r_2}(1+c_{21}) + \frac{f}{K_2^2}(k_{p22}\xi_{0,0}) + \phi_{12}f\frac{1}{K_1}\frac{1}{K_2}(k_{p11}\lambda_{0,0})\right]\right\} + 1 \quad \text{(A43)}$$

if one assumes that cross chain propagations occur much more frequently than chain transfer and chain terminations, it is possible to write

$$\overline{i_T} = \frac{r_1M_1}{M_2} + 1 = r_1f + 1 \quad \text{(A44)}$$

$$\overline{i_S} = \frac{r_2M_2}{M_1} + 1 = \frac{r_2}{f} + 1 \quad \text{(A45)}$$

$$x_1 = \frac{\overline{i_T}}{\overline{i_T}+\overline{i_S}} = \frac{r_1M_1^2 + M_1M_2}{r_1M_1^2 + 2M_2M_1 + r_2M_2^2} = \frac{r_1f^2+f}{r_1f^2+2f+r_2} \quad \text{(A46)}$$

which may be used for the design of the reactor operation conditions. For instance, the minimum block size condition may be defined as the minimum of

$$F = (\overline{i_T}-1)^2 + (\overline{i_S}-1)^2 = \left(\frac{r_1M_1}{M_2}\right)^2 + \left(\frac{r_2M_2}{M_1}\right)^2 = r_1^2f^2 + \frac{r_2^2}{f^2} \quad \text{(A47)}$$

which is placed at

$$f = \sqrt{\frac{r_2}{r_1}}; \quad \overline{i_T} = \sqrt{r_1r_2} + 1; \quad \overline{i_S} = \sqrt{r_1r_2} + 1 \quad \text{(A48)}$$

Therefore, in the case studied, polymers with small average block sizes may be produced, as the product r_1r_2 is approximately equal to 0.1. Equations (A44)–(A48) also show that the internal molecular architecture and composition cannot be manipulated simultaneously, unless it is possible to manipulate the reactivity ratios of the reacting system.